Talanta 97 (2012) 376–381

Contents lists available at SciVerse ScienceDirect

Talanta

journal homepage: www.elsevier.com/locate/talanta

# The dual role of deposited microbead plug (DMBP): A blood filter and a conjugate reagent carrier toward point-of-care microfluidic immunoassay

Chunyu Li, Chong Liu*, Zheng Xu, Jingmin Li

*Key Laboratory for Micro/Nano Technology and System of Liaoning Province, Dalian University of Technology, Dalian, China*

ARTICLE INFO

*Article history:*
Received 3 January 2012
Received in revised form
13 April 2012
Accepted 21 April 2012
Available online 1 May 2012

*Keywords:*
Deposited microbead plug (DMBP)
Blood separation
Reagent storage
Capillary force
Microfluidics

ABSTRACT

To set up a point-of-care whole-blood immunoassay system, sample preparation and on-chip storage of conjugate reagents are indispensable functional units. Here, we merge these functions into a deposited microbead plug (DMBP) to simultaneously play the roles of a blood filter and a conjugate reagent carrier. The DMBP was easily fabricated by the use of natural deposition of beads without the need of weirs. Conjugate reagents (FITC labeled antibodies used here) were incorporated into the DMBP during the assembly of the DMBP. To demonstrate the ability of the DMBP, we constructed a DMBP-based microfluidic chip and used it for the detection of human IgG (hIgG). The DMBP enabled to remove blood cells from whole blood and provide the pure plasma for the downstream on-chip immunoreactions. The release of reconstituted FITC labeled antibodies from the DMBP was controlled in a passive fashion. Dry FITC labeled antibodies retained at least 81% of their activity after 60 days of storage at the room temperature. The DMBP presented here makes an important step towards the development of the self-contained, integrated, sample-to-answer microfluidic chips for point-of-care diagnostics.



## 1. Introduction

Immunoassay based on the specificity of the antibody–antigen reaction is widely used in basic research and clinical diagnostics. Conventional immunoassay is usually done by technicians in the laboratory, involving laborious sample preparation process, multiple pipetting reagent steps, and time-consuming immunoreactions and detection. Point-of-care based immunoassay puts forward the new concept which promises to provide a convenient and immediate test to the untrained user at bedside. To realize this concept, a device which uses small raw samples taken directly from the patient and enables to integrate all the handling steps from sample to result with minimal user intervention would be preferred [1]. On-chip blood separation and reagent pre-storage are indispensable components in point-of-care devices.

Microfluidics with distinct advantages including small sample volumes, rapid results, and integration of multiple laboratory functions onto a single chip become an ideal platform for the point-of-care assays. A number of microfluidic devices for blood separation has been developed using various principles such as filtration [2–11], acoustic force [12,13], centrifugation [14,15], and biomimetics [16–19]. Recently, few cases have fulfilled the on-chip integration of blood separation with downstream analysis. For example, Fan et al. presented a biomarker detection chip on which blood separation based on the Zweifach-Fung effect was integrated [20]. Dimov et al. reported a blood analysis system that utilized blood cell sedimentation to realize on-chip blood separation [21]. Lee et al. performed whole blood immunoassay on a centrifugal microfluidic platform, which extracted plasma from whole blood using centrifugal force generated by the rotation of CD-like chip [22].

Currently, according to the state of reagents, the studies of reagent pre-storage on a microfluidic chip can be divided into two categories: liquid [23,24] and dry power [25,26]. Pre-storage of liquid in glass ampoules provided a method to prevent evaporation of liquid since polymer chip materials, especially PDMS, are permeable to vapor [27]. The glass ampoules filled with the various liquid reagents were placed on a centrifugal microfluidic platform. The on-demand release was realized by the regulation of rotational speed to crush the glass ampoules. Alternative method was to create discrete reagent droplets with the use of immiscible phases [28,29]. Compare with liquid reagents, dry reagents would have a longer life time especially in extreme environmental conditions. Stevens et al. demonstrated on-chip microfluidic immunoassay on the polymer card into which a fibrous pad containing dry labeling antibody was incorporated [30]. Hitzbleck et al. presented a reagent integrator where reagents were loaded by an inkjet spotter and dried in air. This reagent integrator enabled to control the release of reagents [31].

*Abbreviations:* Deposited microbead plug, (DMBP); Human IgG, (hIgG); Bovine serum albumin, (BSA); Goat anti-human IgG, (g-hIgG); Phosphate buffered saline, (PBS); Charge-coupled device, (CCD); Standard deviation, (SD)

* Corresponding author. Tel.: +86 411 84707946; fax: +86 411 84707940.
*E-mail address:* chongl@dlut.edu.cn (C. Liu).

0039-9140/$ - see front matter © 2012 Elsevier B.V. All rights reserved.
http://dx.doi.org/10.1016/j.talanta.2012.04.048

Although some examples fulfill reagent storage or blood separation on the microfluidic platform, most of them still require laborious manual handling or expensive peripheral equipment. Moreover, the integration of these components could dramatically increase complexity and cost of chip fabrication. So, the realization of both functions on a passive microfluidic chip with a simple, low-cost, and non-instrumented method is still a challenge.

In this study, we present the deposited microbead plug (DMBP) combining two functions which not only provides the on-chip separation of whole blood, but also allows the long-term preservation of all required reagents. Based on the previous work utilizing the DMBP to separate blood [32], we further integrate the function of the on-chip reagent storage into the DMBP. Conjugate reagents (FITC labeled antibodies used here) were incorporated into the DMBP during the assembly of the DMBP. The internal porous structures of the DMBP can block blood cells while allow blood plasma to penetrate. The filtered plasma reconstituted dry conjugate reagents pre-stored in the DMBP during it passed through the internal interstices of the DMBP. Capillary forces are used to drive fluids during the assay. The operation for users only needs to drop blood samples at the inlet. The release profile of conjugate reagents was characterized in detail. Dry conjugate reagents stored in the DMBP retained at least 81% of their activities after 60 days of storage at the room temperature. Merging both functions into the DMBP enables to simplify cumbersome immunoassay operations and make the DMBP-based point-of-care devices more portable and robust.

## 2. Experimental section

### 2.1. Fabrication and design of the DMBP-based chip

As schematically shown in Fig. 1, the DMBP-based PDMS chip consists of three elements: the DMBP, the reaction chamber, and the capillary pump. The DMBP is fabricated in the sample inlet by a method of natural deposition of beads. The reaction chamber is 1.5 mm long, 0.25 mm wide, and 50 μm deep. Compared with the reaction chamber, the capillary pump contains many smaller flow paths (see Supplementary data, Fig. S1 for parameters), which enables to increase capillary pressure. The increased capillary pressure facilitates to the elevation of the plasma extraction rate. Moreover, the capillary pump located at the end of the flow path also acts as a waste collector.

The surface-embossed PDMS chip was fabricated by soft lithography technology [33]. Briefly, a SU-8 mold was firstly fabricated using standard photolithography technology. The PDMS precursor and curing agent (Sylgard 184, Dow Corning, USA) were thoroughly mixed in a weight ratio of 10:1 and degassed in vacuum. The curing mixture was poured onto the SU-8 mold to a final thickness of 2.5 mm and cured in an oven for 2 h at 80 °C. The PDMS slab was peeled off from the mold and cut by a knife to make the opening inlet and outlet (at the terminus of the capillary pump). To produce a capillary-driven flow, the surface-embossed PDMS slab was treated by oxygen plasma for 1.5 min, which renders surface of PDMS hydrophilic and reduces the non-specific absorption. Finally, this PDMS slab was placed orthogonally to the antibody strips that were immobilized onto the plain PDMS substrate in advance.

### 2.2. Fabrication of the DMBP and incorporation of conjugate reagents

In this study, we incorporated conjugate reagents into the DMBP during the assembly of the DMBP. Silica beads (Sphere scientific corporation, China) with 4 μm in diameter were used to prepare bead slurry in the conjugate reagent solution containing 1% bovine serum albumin (BSA), 5% trehalose, 200 μg $mL^{-1}$ FITC-conjugated goat anti-human IgG (g-hIgG) in PBS. The end concentration of bead slurry was 100% (W/V). Bead slurry was gently agitated prior to each loading. A drop of bead slurry was loaded on the opening sample inlet. Slurry was drawn into the channel by the capillary force and dried in air at the room temperature. With evaporation of water, beads naturally were deposited onto the channel to form a compact DMBP, while conjugate reagents were deposited onto the surface of beads simultaneously. Although the drying process could be influenced by temperature, humidity, and the concentration of the introduced bead slurry, the drying was rapid and usually completed within 2 min. After the formation of the DMBP, residual beads near the sample inlet were removed carefully. The length of the DMBP was ~1.2 mm, which can be controlled by adjusting the volume of introduced bead slurry.

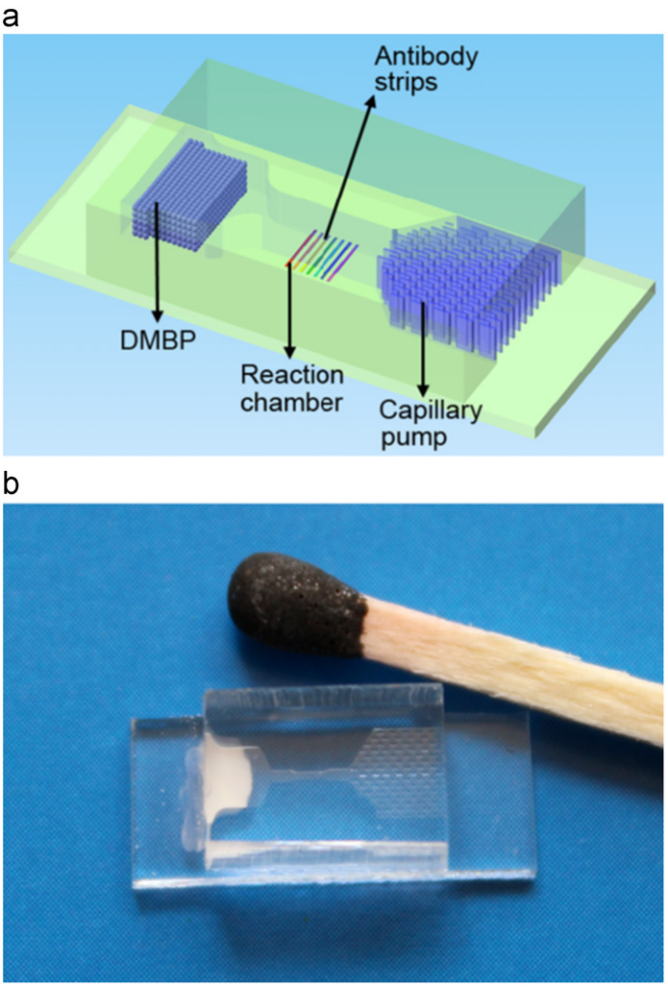


**Fig. 1.** (a) Schematic diagram of a DMBP-based microfluidic chip. This chip contains three elements: the DMBP, the reaction chamber, and the capillary pump. The DMBP is used as a filter for plasma extraction and a carrier for conjugate reagents; the reaction chamber enables to accommodate multiple antibody strips; the capillary pump provides fluid propulsion using capillary force. (b) Photograph of the chip.

### 2.3. Immobilization of antibody strips

The patterning of antibody strips involved the following steps: (1) a pre-fabricated PDMS slab containing parallel microfluidic channels was treated with oxygen plasma, and then incubated in 3% BSA solution for 30 min at the room temperature, rinsed with

ultrapure water (18 MΩ $cm^{-1}$) and dried by $N_2$. Then it was covered over a plain PDMS substrate to form temporally sealed channels; (2) 500 nL of 1 mg $mL^{-1}$ g-hIgG in PBS was injected into the channels where g-hIgG molecules were physically absorbed onto the hydrophobic plain PDMS substrate. The immobilization was carried out at the room temperature for 1 h in a chamber with 100% humidity; (3) PDMS slab was peeled from the plain PDMS substrate after the g-hIgG solution was removed; (4) the plain PDMS substrate surface was blocked for non-specific binding with 3% BSA for 30 min, and then rinsed with ultrapure water and dried by $N_2$.

### 2.4. Assay procedure

10 μl of sheep blood spiked with hIgG was dropped on the sample inlet. The blood permeated the DMBP due to capillary action. The internal pore structures of the DMBP block blood cells while allow plasma to pass through. When the filtered plasma flowed through the internal interstices of the DMBP, dry FITC-conjugated g-hIgG molecules were reconstituted, released from the DMBP, and bound with hIgG. The hIgG–FITC-conjugated g-hIgG complexes were captured by immobilized antibody strips at the reaction chamber. Excess complexes moved past the reaction chamber and flowed into the capillary pump.

### 2.5. Detection and image analysis

The process of blood separation was monitored with a measuring microscope (Olympus STM6) equipped with a charge-coupled device (CCD) camera (Photometrics Coolsnap). Fluorescence signals from immunoassay were detected by an inverted fluorescence microscope (Olympus IX71) equipped with a white–black CCD camera. The collected images were processed and analyzed using Image Pro Plus 6.0 software.

## 3. Results and discussion

### 3.1. Blood separation using the DMBP

The DMBP fabricated by hydrophilic silica beads has a porous structure which enables to impede blood cells while allow blood plasma to pass through. When penetrating the DMBP, the filtered plasma moved into the reaction chamber and finally filled the capillary pump due to the hydrophilic wall of the PDMS channel treated by oxygen plasma. Because of a low flow rate ($\sim$1 nL $s^{-1}$) in this study, the drag force generated by the flow of fluid through the interstices of the DMBP is not big enough to overcome interaction forces between beads and between the bead and the wall of the channel. So, the DMBP enables to remain in its initial configuration during the assay, even without wires or dams to restrict. Fig. 2 showed the process of blood separation using the DMBP. Filtered plasma penetrated the DMBP, flowed through reaction chamber, and finally filled the capillary pump under the action of the capillary force. The average flow rate was $\sim$1.04 nL $s^{-1}$. It was noted that some microbeads detached from the front of the DMBP, but they did not leak into the reaction chamber. No blood cells or beads in the filtered plasma were detected.

### 3.2. The modes for the incorporation of conjugate reagents into the DMBP

Uniform distribution of conjugate reagents in the DMBP is critical for the final performance of immunoassay. Two incorporation modes were investigated. The first mode is to add reagents after the assembly of the DMBP (Fig. 3a). The second mode is to add reagents during the assembly of the DMBP (Fig. 3b). For the first mode, 60 nL of the conjugate reagent solution was dropped onto the sample inlet after the assembly of the DMBP. Due to the hydrophilic porous structures of the DMBP, the reagent solution was sucked into the DMBP spontaneously. As shown in Fig. 3a,

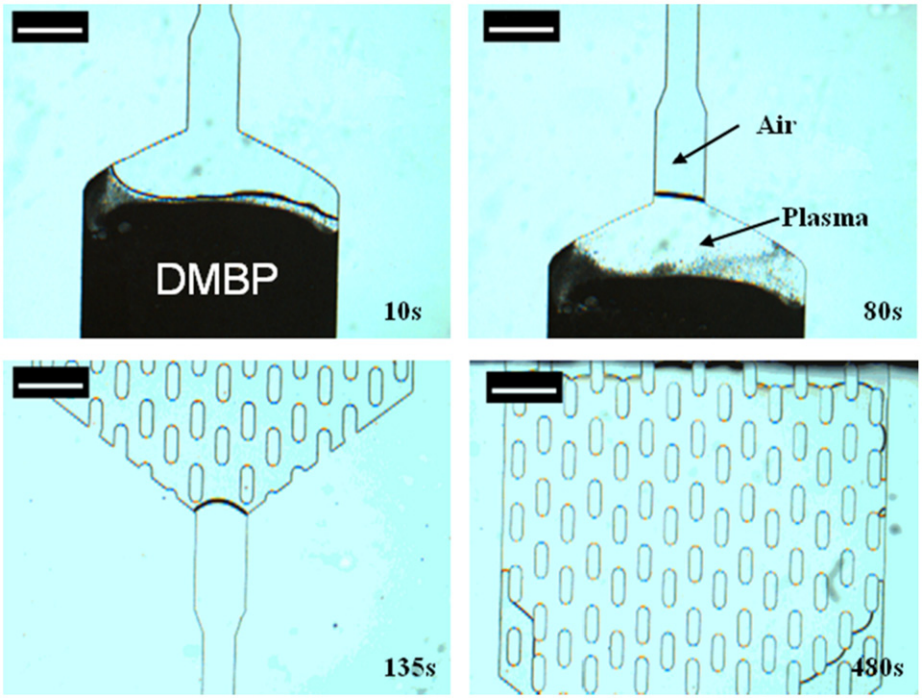


**Fig. 2.** Blood separation in the DMBP-based microfluidic chip. The images were collected per five seconds with the resolution of 640 × 480 pixels. Scale bar represented 500 μm.

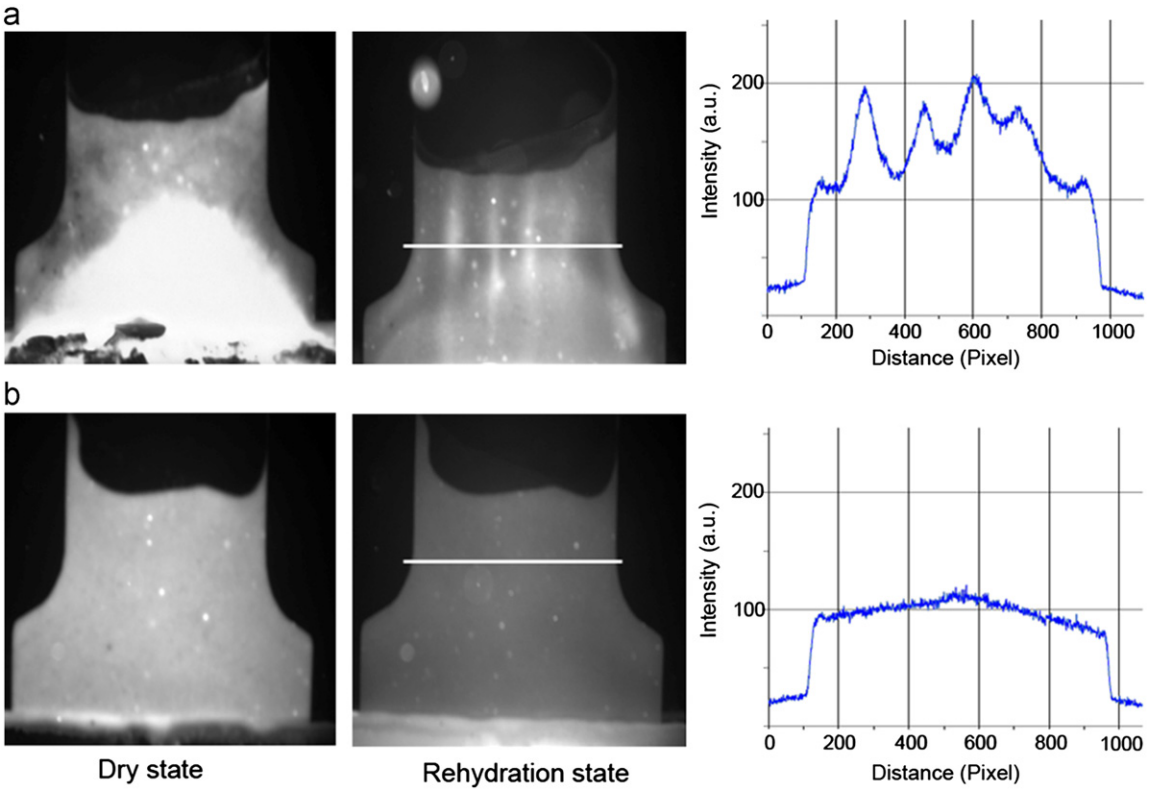


**Fig. 3.** Modes for the incorporation of conjugate reagents into the DMBP. (a) Loading reagents after the DMBP assembly. (b) Loading reagents during the DMBP assembly.

conjugate reagents were distributed non-uniformly within the DMBP, which was manifested by non-uniform fluorescence signals. Moreover, the volume of the introduced solution should be carefully controlled. The excess addition of the solution could lead to the leakage of the solution into the reaction chamber and the contamination of the reaction chamber. For the second mode, silica microbeads were resuspended in the conjugate reagent solution to prepare bead slurry. And then bead slurry was introduced into the channel and dried in air. Because microbeads were premixed with the reagent solution, all the beads were coated with conjugate reagents evenly. The DMBP showed uniform distribution of fluorescence signals. According to these results, the second addition mode of conjugate reagents was selected for the following experiments.

### 3.3. Controlled release of dry conjugate reagents from the DMBP

In this work, another role of the DMBP is to accept conjugate reagents and release them efficiently and reproducibly when the assay is performed. After loading 10 μL of whole blood at the sample inlet, the filtered plasma dissolved the dry conjugate reagents and made them release from the DMBP. The release process was monitored and fluorescence images were collected every 20 s for 800 s (Fig. 4a). In the first ~80 s, no signal was detected because there was a delay for the filtered plasma to penetrate the DMBP and flow into the observation spot. Following a delay, fluorescence intensity increased rapidly and reached the maximum value at 140 s. Then, the fluorescence intensity dropped to ~27% of its maximum value at ~480 s. At this time, the capillary pump was fully filled with the filtered plasma, according to the study of blood separation above. After 480 s, the paper towels were placed on the terminus of the capillary pump to suck the solution continuously. To reduce fluctuations in the flow rate, the paper towels should be wet out before use. At ~800 s, fluorescence intensity was close to background. These results demonstrated that the release of dry reagents from the DMBP can be controlled temporally.

The fluorescence signal growth of capture areas was shown in Fig. 4b and c. 10 μL of whole blood spiked with different concentrations of hIgG (10 μg $mL^{-1}$ and 1 μg $mL^{-1}$) was used. The filtered plasma containing hIgG reconstituted dry FITC-conjugated g-hIgG pre-stored in the DMBP. Dissolved FITC-conjugated g-hIgG was bound with hIgG to form complex. These complexes were captured by immobilized antibody strips at the reaction chamber.

### 3.4. The storage of dry conjugate reagents in the DMBP

The PDMS chip treated by oxygen plasma cannot maintain hydrophilicity for a long time. To investigate the long-term storage stability of dry conjugate reagents, we adopted the off-chip storage. 100% bead slurry containing 1% BSA, 5% trehalose, 200 μg $mL^{-1}$ FITC-conjugated g-hIgG in PBS was dried in air and stored at the room temperature. Prior to using them, bead slurry was restored to the initial concentration in distilled water for fabricating the DMBP. Trehalose added to the conjugate solution is used as a protein stabilizer, which can prevent protein denaturation during solution dehydration and extend the lifetime of dried protein reagents [34]. Moreover, BSA is also introduced into the conjugate solution, which enables to reduce non-specific protein adsorption of microbeads.

The activity of FITC-conjugated g-hIgG was determined using sheep blood spiked with different concentrations of hIgG after 60 days of storage in the dried state. Fig. 5 showed that dry FITC-conjugated g-hIgG preserved at least 81% of their activities after 60 days. It was noted that fluorescence signals at a higher concentration of hIgG (100 μg $mL^{-1}$) were lower than those at a lower concentration (10 μg $mL^{-1}$). This result attributes to hook

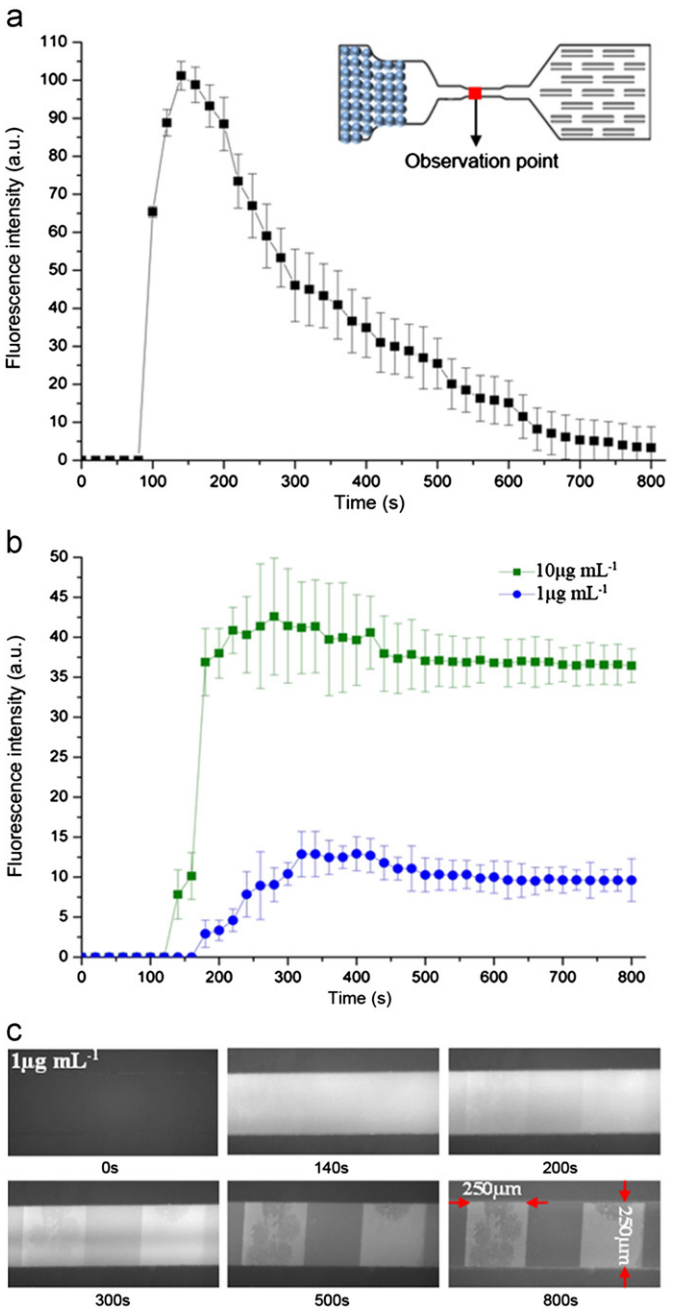


**Fig. 4.** (a) Profile of the release of dry conjugate reagents from the DMBP. The inset shows the location of the observation point. (b) The growth of fluorescence signals of reaction areas. The fluorescence intensity of the reaction area was calculated by subtracting background noise which was measured from the zone between the reaction areas from the grayscale values of the reaction area. (c) Fluorescence image profiles. Error bar represented $\pm 1$ SD ($n=3$).

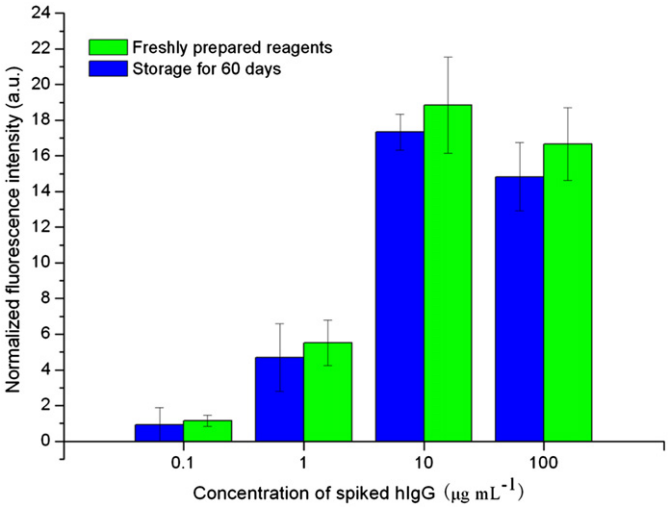


**Fig. 5.** Comparison of activity of freshly prepared reagents and reagents stored for 60 days. To avoid signal saturation, exposure time was varied between 1 s and 5 s. The normalized fluorescence intensity was calculated as $I=(G-G0)/t$. $I$ represents the normalized fluorescence intensity; $G$ and $G0$ are the averaged grayscale values of the reaction area and the zone between the reaction areas, respectively; $t$ is the exposure time. Error bar represented $\pm 1$ SD ($n=3$).

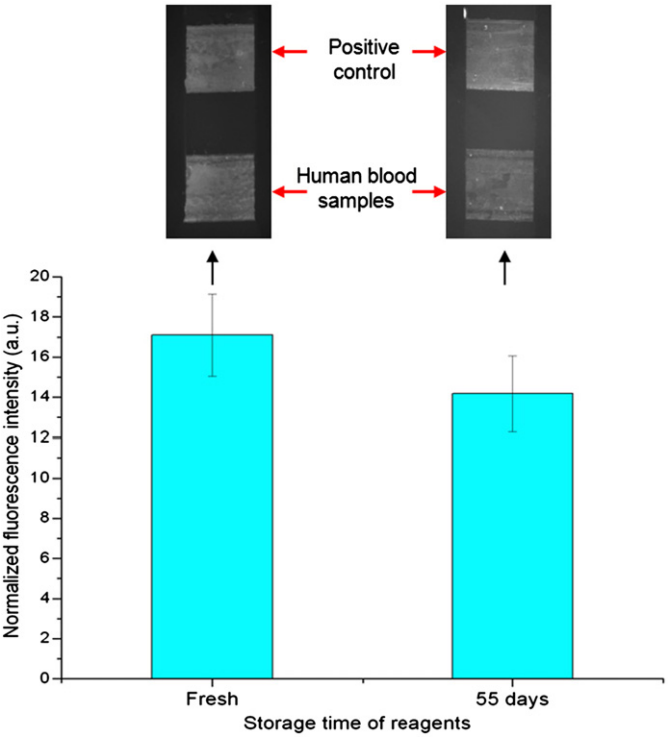


**Fig. 6.** Detection of hIgG from human blood using the DMBP-based chip. The fluorescence images included detection signal and positive control. Error bar represented standard deviation ($n=3$).

effect [35]. Excess analyte molecules bind to all available sites on both the immobilized capture antibody as well as labeled detection antibody and thereby prevent the sandwich-formation.

Fig. 6 showed the detection of hIgG from human blood. Human blood samples were diluted 1:1000 in PBS solution before the assay. The fluorescence images showed a specific signal for human blood samples and a positive control signal on the same chip where FITC-conjugated g-hIgG binds to hIgG on the PDMS surface. This result indicated the DMBP-based chip with the dual functions has the ability to deal with the analysis of real samples.

## 4. Conclusion

In this work, we demonstrate the ability of the DMBP to extract plasma from a small-volume of blood sample like a finger prick and to accept and release conjugate reagents efficiently and reproducibly when the assay is run. As a sample preparation element, the DMBP has some features: (1) the easy and rapid fabrication; (2) the requirement of little space; (3) simple to use; and (4) easy to integrate with other microfluidic elements. We believe that the DMBP-based microfluidic chip combined

with blood separation and on-chip storage of reagents has the potential to become a sample-to-answer, point-of-care platform for blood diagnostics. Toward this goal, there are still some needs to be done in the further work. The more stable surface hydrophilic modification methods could be adopted to improve shelf life of the PDMS chips. Hydrophilic thermoplastic could also be used as a substitute, considering its low cost and possibility of mass production.

## Acknowledgments

This work was supported by the National Natural Science Foundation of China (nos. 20890024, 91023017, 91023046, 51105060), the National High Technology Research and Development Program of China (no. 2012AA040406), and the National Basic Research Program of China (no. 2007CB714502).

## Appendix A. Supplementary data

Supplementary data associated with this article can be found in the online version at http://dx.doi.org/10.1016/j.talanta.2012.04.048

## References

[1] L. Gervais, N. de Rooij, E. Delamarche, Adv. Mater. 23 (2011) H151–H176.
[2] J. Moorthy, D.J. Beebe, Lab Chip 3 (2003) 62–66.
[3] Y.C. Kim, S.H. Kim, D. Kim, S.J. Park, J.K. Park, Sensor. Actuat. B: Chem. 145 (2010) 861–868.
[4] H.M. Ji, V. Samper, Y. Chen, C.K. Heng, T.M. Lim, L. Yobas, Biomed. Microdevices 10 (2008) 251–257.
[5] G. Maltezos, J. Lee, A. Rajagopal, K. Scholten, E. Kartalov, A. Scherer, Biomed. Microdevices 13 (2011) 143–146.
[6] J. Moorthy, G.A. Mensing, D. Kim, S. Mohanty, D.T. Eddington, W.H. Tepp, E.A. Johnson, D.J. Beebe, Electrophoresis 25 (2004) 1705–1713.
[7] J.S. Shim, A.W. Browne, C.H. Ahn, Biomed. Microdevices 12 (2010) 949–957.
[8] T. Tachi, N. Kaji, M. Tokeshi, Y. Baba, Anal. Chem. 81 (2009) 3194–3198.
[9] S. Thorslund, O. Klett, F. Nikolajeff, K. Markides, J. Bergquist, Biomed. Microdevices 8 (2006) 73–79.
[10] V. VanDelinder, A. Groisman, Anal. Chem. 78 (2006) 3765–3771.
[11] C. Xing, C. Da.Fu, L. Chang Chun, L. Hui, Sensor. Actuat. B: Chem. 130 (2008) 216–221.
[12] A. Lenshof, A. Ahmad-Tajudin, K. Jaras, A.M. Sward-Nilsson, L. Aberg, G. Marko-Varga, J. Malm, H. Lilja, T. Laurell, Anal. Chem. 81 (2009) 6030–6037.
[13] F. Petersson, A. Nilsson, C. Holm, H. Jonsson, T. Laurell, Analyst 129 (2004) 938–943.
[14] S. Haeberle, T. Brenner, R. Zengerle, J. Ducree, Lab Chip 6 (2006) 776–781.
[15] M. Amasia, M. Madou, Bioanal. 2 (2010) 1701–1710.
[16] M. Faivre, M. Abkarian, K. Bickraj, H.A. Stone, Biorheol. 43 (2006) 147–159.
[17] E. Sollier, M. Cubizolles, Y. Fouillet, J.L. Achard, Biomed. Microdevices 12 (2010) 485–497.
[18] S. Yang, A. Undar, J.D. Zahn, Lab Chip 6 (2006) 871–880.
[19] A.I. Rodriguez-Villarreal, M. Arundell, M. Carmona, J. Samitier, Lab Chip 10 (2010) 211–219.
[20] R. Fan, O. Vermesh, A. Srivastava, B.K.H. Yen, L.D. Qin, H. Ahmad, G.A. Kwong, C.C. Liu, J. Gould, L. Hood, J.R. Heath, Nat. Biotechnol. 26 (2008) 1373–1378.
[21] I.K. Dimov, L. Basabe-Desmonts, J.L. Garcia-Cordero, B.M. Ross, A.J. Ricco, L.P. Lee, Lab Chip 11 (2011) 845–850.
[22] B.S. Lee, J.N. Lee, J.M. Park, J.G. Lee, S. Kim, Y.K. Cho, C. Ko, Lab Chip 9 (2009) 1548–1555.
[23] J.L. Garcia-Cordero, F. Benito-Lopez, D. Diamond, J. Ducree, A.J. Ricco, in: Proceedings of the IEEE 22nd International Conference on Micro Electro Mechanical Systems, MEMS 2009, 2009.
[24] K. Abi-Samra, R. Hanson, M. Madou, R.A. Gorkin, Lab Chip 11 (2011) 723–726.
[25] E. Garcia, J.R. Kirkham, A.V. Hatch, K.R. Hawkins, P. Yager, Lab Chip 4 (2004) 78–82.
[26] D. Chen, M. Mauk, X. Qiu, C. Liu, J. Kim, S. Ramprasad, S. Ongagna, W.R. Abrams, D. Malamud, P.L.A.M. Corstjens, H.H. Bau, Biomed. Microdevices 12 (2010) 705–719.
[27] J. Hoffmann, D. Mark, S. Lutz, R. Zengerle, F. von Stetten, Lab Chip 10 (2010) 1480–1484.
[28] D.L. Chen, R.F. Ismagilov, Curr. Opin. Chem. Biol. 10 (2006) 226–231.
[29] V. Linder, S.K. Sia, G.M. Whitesides, Anal. Chem. 77 (2005) 64–71.
[30] D.Y. Stevens, C.R. Petri, J.L. Osborn, P. Spicar-Mihalic, K.G. McKenzie, P. Yager, Lab Chip 8 (2008) 2038–2045.
[31] M. Hitzbleck, L. Gervais, E. Delamarche, Lab Chip 11 (2011) 2680–2685.
[32] C. Li, C. Liu, Z. Xu, J Li, Microfluid. Nanofluid. http://dx.doi.org/10.1007/s10404-011-0911-5, in press.
[33] D.C. Duffy, J.C. McDonald, O.J.A. Schueller, G.M. Whitesides, Anal. Chem. 70 (1998) 4974–4984.
[34] J.H. Crowe, J.F. Carpenter, L.M. Crowe, Annu. Rev. Physiol. 60 (1998) 73–103.
[35] S.A. Fernando, G.S. Wilson, J. Immunol. Methods 151 (1992) 47–66.